Robotica (2008) volume 26, pp. 667–677. © 2008 Cambridge University Press
doi:10.1017/S0263574708004281 Printed in the United Kingdom

# Robot multiple contact control

Jaeheung Park*† and Oussama Khatib‡

†*Stanford Artificial Intelligence Laboratory. Address: Gates Building Room 122, 353 Serra Mall #146, Stanford, CA 94305-9010.*
‡*Stanford Artificial Intelligence Laboratory. Gates Building Room 144, 353 Serra Mall #146, Stanford, CA 94305-9010.*

(Received in Final Form: February 7, 2008. First published online: March 27, 2008)

**SUMMARY**
This paper addresses the problem of contact force control for multiple contacts distributed over multiple links in a robot. This is of importance when performing complex tasks in unstructured environment, particularly in humanoid robot applications. The proposed multicontact control framework provides a new way of defining the operational space coordinates, which facilitates the specification of multiple contact control. The contact force space on multiple links is constructed as an operational space for the highest priority task. Motion control, given lower priority, can be executed using the rest of degree of freedom within the null-space of the force control. The dynamic control structure, then, provides a means to control each contact force and motion independently. This dynamic decoupling enables each contact force controller to utilize linear control theories. In particular, the contact force controllers adopt full state feedback control and estimation methods to produce robust performance with respect to modeling and parameter uncertainties. The effectiveness of the multiple contact control framework was demonstrated using a PUMA560 manipulator, with multiple contacts on the end-effector and third link. The demonstrated tasks involved controlling each of the contact forces with null-space motion.

KEYWORDS: Multiple contacts; Multiple links; Force control; Motion control; Humanoid; Manipulator.

## 1. Introduction

Recent developments in humanoid robotics have ignited an expectation for these robots to begin operating in human environments. While many mechanically sophisticated humanoids have been designed, there still exists the challenge of providing these robots with appropriate control frameworks to cope with complex and unstructured environments. These environments differ greatly from traditional settings such as factory floors and assembly lines. In addition to the increasing complexity of the intended operating environment, the robots themselves have evolved into more complex and highly articulated systems.

Tasks for high DOF robots in complex environments often involve multiple contacts over multiple links (Fig. 1). These tasks require precise and robust control of contact forces as well as motion for the entire robot. Most control algorithms, however, have been developed for the execution of tasks only at the end-effector. This paper proposes a new approach on how to specify and execute tasks in the case of multiple contact over multiple links with the environment.

Most of the research in motion and force control strategy has dealt with contact at the end-effector of the manipulator, since the manipulators were specifically designed to only interact with the environment at the tip.[5,26,29] Compliant frame selection matrices were introduced in ref. [22] to select *compliant* directions to interact with the environment, and later Khatib [11] presented generalized selection matrices to describe the decomposition of the end-effector space in the contact frame. These selection matrices, however, are limited to orthogonal decomposition at the control point of the end-effector. In general, the contact force space and motion space of the end-effector may not be orthogonal to each other. This problem has been discussed by refs. [3, 8, 14, 18, 28], where more general kinematic contact models have been proposed. However, these contributions are still specifically focused on contacts at the end-effector.

While substantial research has addressed contact at the end-effector, much less research has addressed the control of multiple contacts on multiple links. Liu *et al.* [15] present an adaptive control approach for multiple geometric constraints using joint-space orthogonalization. Using the geometric constraints, the joint velocity commands are composed for contact force and motion control, separately. However, this approach does not provide a decoupled control structure for each contact, and does not allow to consider different models of the contact environment. A unified task specification approach is presented based on constraints in ref. [25]. Interaction forces are introduced as dynamic constraints and different control approaches are presented. Among them, torque based control is explained but it does not deal with the issue of coupling effect among interaction forces themselves and motion control.

On the other hand, robots having multiple contacts have been investigated in the field of grasping and whole arm manipulation.[2,16,24,30] Multiple branches of the robot, such as fingers, make contacts with an object to manipulate or support the object. Also other parts of the links, such as palm, contribute to it. The focus of the research has been the control issue of the handled object and kinematics to generate required contact forces.

*Corresponding author. E-mail: park73@robotics.stanford.edu

Fig. 1. Humanoid robot experiencing multiple contacts with a complex human environment.

In this paper, we present a task specification approach and control framework for multiple contacts over multiple links. It is based on our earlier work[19] and experimental data presented in refs. [18,19]. Our attention is more on the control issue of a robot than an object, which mainly differs from the work on grasping: how to provide a control structure not only for contact force but also for motion tasks of the robot. In a general case, the contact environment can also be multiple objects. Our proposed approach employs a new way of defining operational space with contact normals at all contacts over the links.

The hybrid motion/force control divides the end-effector control into motion and force control using selection matrices.[11] This approach cannot be directly generalized to the case of contacts at multiple links. The composition of the operational space coordinates for all the contact links and the associated selection matrices cannot provide a control structure for either contact force or motion because the resulting operational space for both contact force and motion would easily result in having larger degree of freedom than the robot as a whole robot. The new approach proposed in this paper is to give a higher priority to contact force control since this is the most critical aspect during interaction with the environment. An efficient way of specifying this contact force control is to construct each operational space coordinate as the normal force direction of the corresponding contact point, forming the minimal operational space coordinates. The motion control is then composed in the null-space of the contact force control. This approach provides an effective method of task specification as well as a control framework to deal with multiple contacts.

The dynamics of the operational space coordinates are then obtained by projecting the robot dynamics into the corresponding space. Additionally, an environment model is specified to obtain the dynamics of contact forces. Control torques are chosen to compensate for the dynamics, resulting in a linearized second-order system for each contact force.[9,11] This framework allows the use of any linear controller at the level of the decoupled system. The nonlinear dynamic decoupling method for robots is effective since inaccuracies of the model used for decoupling have only a minor effect compared to the unknown disturbances, unmodeled friction, and parameter errors in the environment model, which are already being dealt with by the linear controller.

Among linear control theories, the active observer design (AOB)[6] is chosen to improve the robustness with respect to disturbances. The AOB design uses a Kalman observer and full state feedback with input disturbance estimation;[10] thus, it realizes a model reference control approach,[1] which implements controllers to adaptively follow the desired model of the system response rather than simply tracking a reference trajectory.

The main contribution of this paper is the development of a new approach in the composition of the control variables (the operational space coordinates), which provides a control structure in the multi-contact situation. This was not possible in previous hybrid motion/force control methods.[8,11,23] Then, full state feedback control with Kalman observer (AOB) was implemented at the level of linearized systems. The overall control structure exploits the dynamic model of the system; thus, it enables us to use the Kalman estimator at the level of each linearized system, which corresponds to each contact force.

This new approach has been developed for application in high DOF robots, such as humanoids making contacts at multiple links (Fig. 1). Due to hardware limitations, experiments were conducted on a PUMA560 manipulator to demonstrate the performance of the multi-contact force control approach. To our knowledge, it is the first demonstration of a multiple contact control framework over multiple links on a physical robotic system. Multiple contact control on one link and multiple links was demonstrated to show the effectiveness of the multiple contact force control framework. During the multi-contact demonstration, the contact points were moving, i.e., sliding, on the surface since the motion was also controlled in the null-space of the contact force control.

## 2. Control Framework for Multicontact Force Control

The hybrid motion/force control of the end-effector uses a selection matrix, which selects the force and motion control directions in an orthogonal frame.[11,22] In Fig. 2(a), a robot is in contact with a horizontal plane. Therefore, the vertical direction can be chosen as a force control direction and the others as motion control directions using a selection matrix. It has been further generalized so that arbitrary force and motion at the end-effector (Fig. 2(b)) can be composed.[8] In dealing with multiple contacts, the corresponding multiple links can be chosen to concatenate the 6 dimensional operational coordinates of the each link[23] while a selection

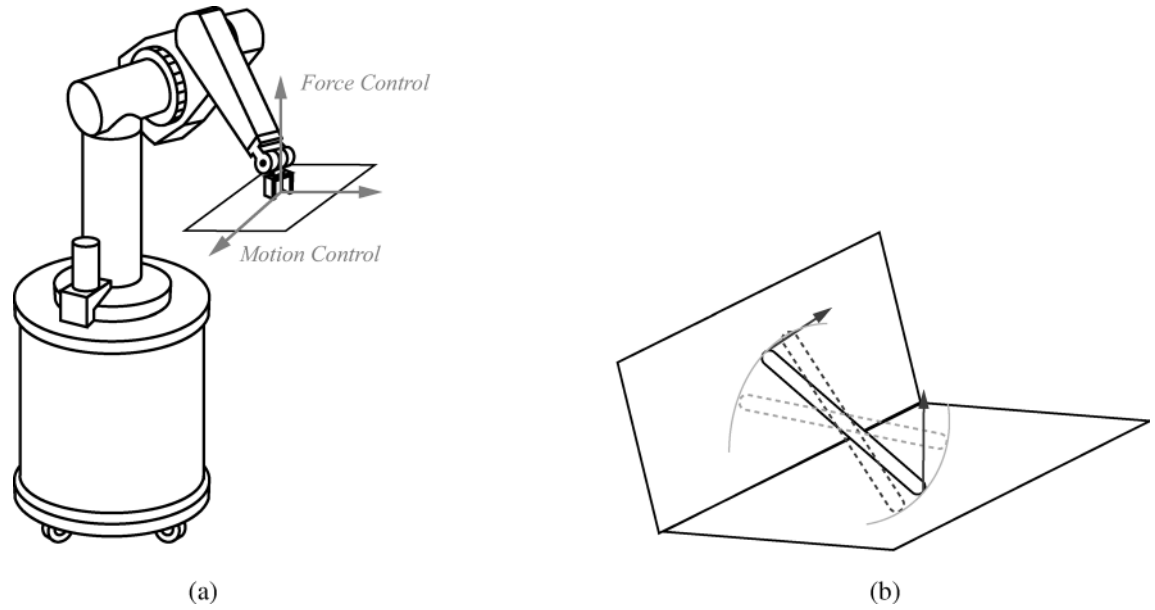


Fig. 2. (a) Motion and force control direction of the end-effector in contact with a horizontal plane. A selection matrix can be determined to select the force and motion control directions. (b) End-effector in multiple contacts with the environment, where motion and force space are not orthogonal.

matrix can be used for force and motion control at each link. This approach, however, may result in operational space coordinates which are larger than the degrees freedom of the robot. For example, two link contact situation would require 12 dimensional coordinates. Among them, force and motion control would be decided by selection matrices. The motion or force control cannot be both controlled appropriately if the robot has less than 12 degrees of freedom.

In most interactions with the environment, contact force control has higher priority since it is closely related to the safety of the robot, environment, and human. A new approach is proposed based on this priority. The goal is to construct the operational space using the contact force space such that the contact force control can be achieved within the degrees of freedom of the manipulator. This is the main contribution of the paper; unlike previous approaches it can be expanded to multiple contacts, with the remaining degrees of freedom of the robot utilized for motion control.

### *2.1. Operational space coordinates using contact normals*

Given the contact position and configuration of a link, the corresponding Jacobian and contact normal vector can be defined. In the case of point contact as illustrated in Fig. 3, the Jacobian corresponds to the point of contact and the contact normal vector is a unit vector normal to the contact surface. The Jacobian and contact normal vector for the $i$th contact are denoted as $J^i$ and $n_c^i$. The Jacobian of the operational space coordinate is defined as

$$J_c^i = {n_c^i}^T J^i. \tag{1}$$

The instantaneous velocity of the coordinate is denoted as $\vartheta_c^i$ later in the paper.

For $m$ contacts over multiple links, the Jacobian for the operational space coordinates is obtained by concatenating these Jacobians for each contact.

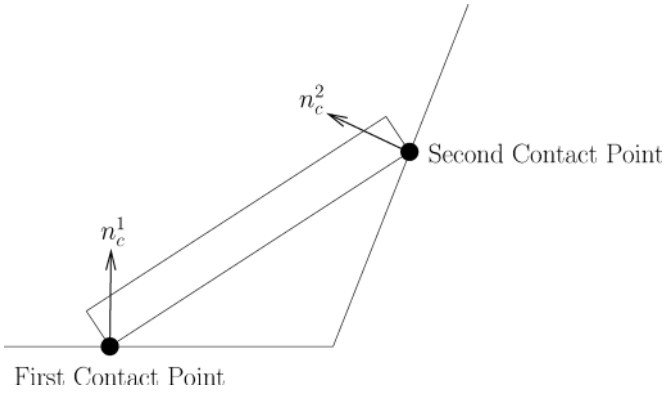


Fig. 3. Multi-contact on a link. $n_c^1$ and $n_c^2$ are unit vectors normal to the contact surfaces, respectively.

$$J_c = \begin{pmatrix} J_c^1 \\ J_c^2 \\ \vdots \\ J_c^m \end{pmatrix}. \tag{2}$$

Similarly, a concatenation of $\vartheta_c^i$ vectors forms the instantaneous velocity of the operational space coordinate, $\vartheta_c$, and a concatenation of $f_c^i$ forms contact force vector, $f_c$.

A unit vector, $n_c^i$, can be used to describe contact moment. Figure 4 illustrates different kinds of rigid body contacts between a robot link and environment. When it is a line contact (Fig. 4 (b)), one of the $n_c^i$ vectors would be the unit vector for the moment about the $x$-axis, in which the rotation of the contact link is constrained. For a plane contact (Fig. 4 (c)), the $n_c^i$ vectors would represent the contact normal

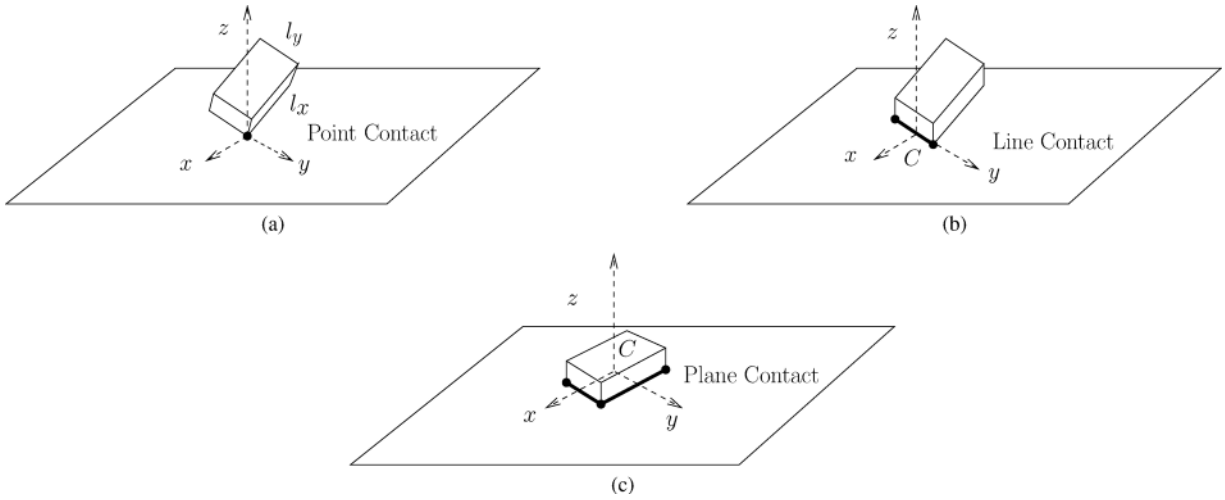


Fig. 4. Rigid body contact. (a) Point contact (b) Line contact (c) Plane contact.

force direction, along the $z$-axis, and moment directions about $x$ and $y$ axes.

Generally, the degrees of freedom of contact forces/moments that can be controlled is limited by the number of joint actuators. The maximum number of contact forces that can be controlled by the six DOF PUMA560 robot is six. Consequently, the number of controllable contact forces on a specific link is limited by the degrees of freedom. For example, the maximum number of contacts that can be controlled at the first link of the PUMA560 robot is only one because the link has one degree of freedom. The second link, therefore, has two. In addition, the directions of the controllable contact force are limited by the kinematics of the joints connected to the contact link. These limitations are due to the kinematic properties of the robot without regard to any specific control framework. The contact forces to be controlled in this paper are assumed to be chosen within the limited contact force space. Therefore, the Jacobian, $J_c$ for PUMA560 has less than or equal to six rows.

### 2.2. *Dynamics and control of the robot in contact*

The equations of motion for manipulators are of the form

$$A(q)\ddot{q} + b(q,\dot{q}) + g(q) + J_c^T(q) f_c = \Gamma, \tag{3}$$

where $q$, $A(q)$, $b(q,\dot{q})$, $g(q)$, and $\Gamma$ are the vector of joint angles, the mass/inertia matrix, the Coriolis/centrifugal torque, the gravity torque in joint space, and the vector of joint torques, respectively.

The joint torque vector, $\Gamma$, is chosen to be composed of the torque for contact force control, and the null space torque:

$$\Gamma = J_c^T F_c + N_c^T \Gamma_0, \tag{4}$$

where the first term $J_c^T F_c$ is the control torque for the contact force control and the second term $N_c^T \Gamma_0$ is the torque in the null space of the contact force control. The equation of motion for $\vartheta_c$ is then obtained by projecting Eq. (3) and (4) into the operational space using $\bar{J}_c^T$,

$$\Lambda_c(q)\dot{\vartheta}_c + \mu_c(q,\dot{q}) + p_c(q) + f_c = F_c, \tag{5}$$

where

$$\Lambda_c^{-1}(q) = J_c(q)A^{-1}(q)J_c^T(q) \tag{6}$$

$$\bar{J}_c^T(q) = \Lambda_c(q)J_c(q)A^{-1}(q) \tag{7}$$

$$N_c^T = I - J_c^T \bar{J}_c^T \tag{8}$$

$$\mu_c(q,\dot{q}) = \bar{J}_c^T(q)b(q,\dot{q}) - \Lambda_c(q)\dot{J}(q)\dot{q} \tag{9}$$

$$p_c(q) = \bar{J}_c^T(q)g(q). \tag{10}$$

Equation (5) has the same structure as the dynamics of the end-effector using the operational space control framework.[11] However, the operational space in this paper does not correspond to the dynamics of one link or specific links but corresponds to the contact normals over multiple links. That is, this equation describes the dynamics of the contact force/moment space over the entire robot.

The control force, $F_c$, in Eq. (5) can be designed by compensating for the dynamic effects with the estimates of the matrices, $\hat{\Lambda}_c(q)$, $\hat{\mu}_c(q,\dot{q})$, $\hat{p}_c(q)$, and $\hat{f}_c$.

$$F_c = \hat{\Lambda}_c(q) f_c^* + \hat{\mu}_c(q,\dot{q}) + \hat{p}_c(q) + \hat{f}_c. \tag{11}$$

The resulting equations of motion form the decoupled unit mass system for each contact.

$$\dot{\vartheta}_c = f_c^*. \tag{12}$$

$$\text{i.e.,} \quad \dot{\vartheta}_{c,i} = f_{c,i}^*, \tag{13}$$

where $i$ denotes each contact.

Having the decoupled system for each contact, the control input, $f_c^*$, for contact force control should be composed using the relation between the motion and contact force. In practice, it is difficult to identify a precise mathematical model for the actual contact environment. Therefore, there is a trade-off in the modeling of this contact environment. A complicated model could be problematic in terms of the estimation of the parameters and use of the model in the control. In this paper, a simple spring model[12] is used for the controller design. In this case the environment is assumed to have a constant stiffness.

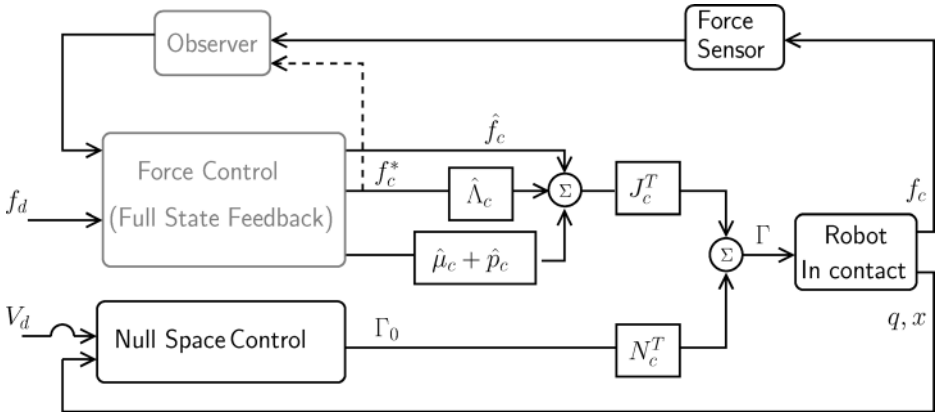


Fig. 5. A block diagram of the contact force control framework for a manipulator, where the Active Observer (AOB) design is implemented for force control. The observer in the AOB design includes a state for input disturbance and the estimate of this state will be directly compensated for in addition to the full state feedback.

Although this model seems too simple to represent the environment, it captures the important characteristic that contact force on most passive objects increases with deflection.

A higher order model for passive environments is a second-order model with mass, damping, and stiffness. The linear spring model is a special case of this model. When the stiffness of the contact object is identified, adding a mass property to the model makes the system slower. Therefore, the simple linear spring model can be considered a conservative model in terms of stability. The use of a linear spring model on the actual second-order system may decrease the performance. So, the proposed approach is to first utilize the stiffness model and design a controller, then, compensate for the modeling errors using an adaptive controller with AOB.

For each contact $i$, we use the stiffness model

$$\dot{f}_{c,i} = k_{s,i}\vartheta_{c,i}, \tag{14}$$

where $f_{c,i}$ is the $i$th contact force. The term, $\vartheta_{c,i}$, is the instantaneous velocity in the contact normal direction and $k_{s,i}$ is the $i$th contact environment stiffness.

With this model and Eq. (13), the resulting dynamics for each contact force, $i$, are

$$\ddot{f}_{c,i} = k_{s,i} f_{c,i}^*. \tag{15}$$

The control input, $f_{c,i}^*$, can now be computed using any linear control method. Among them is a full state feedback control with estimation of input disturbance, which fits well with the proposed control framework. This controller is explained in Section 3.

### *2.3. Motion control in the null space*

The null space control torque, $\Gamma_0$, in Eq. (4) is used for motion control. The dynamically consistent null space projection matrix, $N_c^T$, projects the torque, $\Gamma_0$, into the null space of the contact forces; thus, the contact forces are not affected by $\Gamma_0$.

Having the task-posture decomposition control structure for the contact force and motion control, the task consistent dynamic equation for motion control can be obtained.[13] The dynamic equation with the control structure is

$$A(q)\ddot{q} + b(q,\dot{q}) + g(q) + J_c^T(q) f_c = J_c^T F_c + N_c^T \Gamma_0. \tag{16}$$

We define the operational space coordinate for motion and the corresponding Jacobian is denoted as $J_m$.

$$\vartheta_m = J_m \dot{q}. \tag{17}$$

Control torque for motion, $\Gamma_0$, is thus chosen as $J_m^T F_m$ to apply control force, $F_m$, in the null space. Then, the dynamic equation in the motion space is obtained by projecting the joint space dynamics into the motion space. This projection can be performed by pre-multiplying Eq. (16) by $\bar{J}_{m,c}^T(q)$:

$$\Lambda_{m,c}\dot{\vartheta}_m + \mu_{m,c} + p_{m,c} + \bar{J}_{m,c}^T J_c^T f_c = \bar{J}_{m,c}^T J_c^T F_c + F_m, \tag{18}$$

where

$$\Lambda_{m,c}^{-1}(q) = J_m(q)A^{-1}(q)N_c^T J_m^T(q) \tag{19}$$

$$\bar{J}_{m,c}^T(q) = \Lambda_{m,c}(q)J_m(q)A^{-1}(q) \tag{20}$$

$$\mu_{m,c}(q,\dot{q}) = \bar{J}_{m,c}^T(q)b(q,\dot{q}) - \Lambda_{m,c}(q)\dot{J}_m(q)\dot{q} \tag{21}$$

$$p_{m,c}(q) = \bar{J}_{m,c}^T(q)g(q). \tag{22}$$

Note that this dynamic equation of motion is consistent with the task dynamics. That is, the control force $F_m$ is applied to the null-space of the contact force control. Any torque components that may affect the contact force control will be eliminated by the null-space projection matrix, $N_c^T$.

Based upon Eq. (18) and the composed control force, $F_c$, for the contact force control, the control force in motion control can be computed as

$$F_m = \hat{\Lambda}_{m,c} f_m^* + \hat{\mu}_{m,c} + \hat{p}_{m,c} + \bar{J}_{m,c}^T J_c^T \hat{f}_c - \bar{J}_{m,c}^T J_c^T F_c, \tag{23}$$

resulting in a unit mass system for motion, if the motion control can be executed in the null-space of the force control.

$$\ddot{x}_m = f_m^*. \tag{24}$$

The total torque to be applied to the robot is

$$\Gamma = J_c^T F_c + N_c^T J_m^T F_m. \tag{25}$$

The block diagram of the overall control structure is shown in Fig. 5, where the null space control is used for motion control: thus, $\Gamma_0 = J_m^T F_m$.

*2.4. Discussion on control issue of contact force and motion*

The rank of the Jacobian, $J_c$, determines if all the specified contact forces are controllable simultaneously or not. In the case the rank is deficient, $\Lambda_c^{-1}$ in Eq. (6) becomes a singular matrix. It means not all the contact forces can be controlled. That is, control for some of the contact forces are conflicting. There can be different ways of resolving the situation. Least important contact forces could be eliminated from the task among the conflicting contact forces. Or damped pseudo inverse approach can be applied to obtain $\Lambda_c$ matrix.[17,27] This method compromises their performances among the conflicting contact forces. In ref. [4] singular directions are removed from control near singular configurations and the null space motion is used for the control along the singular directions. This is the same issue for the motion control and similar approaches could be applied in dealing with $\Lambda_{m,c}^{-1}$. However, the use of the null-space projection matrix, $N_c^T$, guarantees force control when the motion control conflicts with it.

## 3. Contact Force Control with Input Disturbance Estimation

A common approach for contact force control uses a proportional-integral (PI) controller with damping based on the velocity of the end-effector. One of the main difficulties with this approach involves hard contact. In this case, the dynamics of contact with the environment are already very fast, so there is a limitation in the proportional gain that can be employed. Thus, the proportional gain must be kept small, which in practice results in large steady state error. This error can be reduced by adding integral control; however, this is problematic since it may adversely affect the stability of the system.

In addition to this difficulty associated with classical PI controllers, the stiffness of the environment is difficult to identify and may even change during contact when deflection occurs. Classical PI controllers cannot deal with these difficulties since they do not account for uncertainties in the system. These facts motivate a force control strategy which employs an observer that can account for uncertainties in a systematic way.

Active Observers (AOB)[6] use a modified Kalman estimator with an additional state, called an active state. The active state is the estimate of the disturbance to the input of the system. Full state feedback is implemented with estimated states that correspond to the contact force and the derivative of the contact force. In addition, the estimated input disturbance (active state) is directly subtracted from the input to compensate for the error. This AOB method is best applied to systems which can be modeled as linear systems with input disturbance. The linearized contact force control system is one such system. In this case feedback linearization is achieved through the use of the operational space formulation. The contact environment is approximated as a spring model and as such modeling uncertainties need to be considered. In addition to these modeling uncertainties most robots cannot accurately provide the commanded torque to the system and this mismatch between commanded torque and actual torque can be treated as an input disturbance. The details for implementation can be found in ref. [7, 20].

## 4. Experiments

The control framework has been developed for a general robot, especially one with high DOF and a branching mechanism, such as a humanoid robot. Due to hardware limitations, experimental demonstration was done using a PUMA560 robot. The robot has six degrees of freedom. Therefore, its possible contact and motion tasks were limited by its kinematics and degrees of freedom.

A PUMA560 manipulator was connected to a PC (running the QNX operating system) through a TRC205 amplifier package from the Mark V Corporation. This setup allowed a user to program joint torques or motor currents as inputs to the robot. The servo rate of the controller for the PUMA560 robot was 500 [Hz]. A JR3 force sensor with 6 axis measurements was mounted on the wrist of the manipulator to measure contact forces at the end-effector.

The experiments have been conducted to demonstrate the effectiveness of the control framework and performance of the contact force and motion control. The first set of experiments was for multiple contacts at the end-effector. The multiple contact force control over multiple links was implemented in the second set of experiments.

*4.1. Multiple contacts at the end-effector*

The system setup, represented in Fig. 6, consisted of a PUMA robot, a table, and a vertical board. The vertical board had a 90° angle with the table. As can be seen in Fig. 6, two rigid bars at the end-effector had contacts with the table and the vertical board. Contact force control was for the normal contact forces at each contact: one with the table and the other with the vertical board. The contact force with the table was in the $z$-direction and the one with the vertical board was in the $y$-direction (Fig. 6). Motion control was performed within the remaining four DOF after controlling the two contact forces. The tasks were to maintain the orientation of the end-effector, which was three-DOF task, and to control the wrist point in the $x$-direction, one-DOF task. The contact Jacobian, $J_c$, consists of two rows. The first row corresponds to the normal contact force with the table. This was obtained by computing the Jacobian for the contact point and then selecting the row corresponding to the $z$-direction. The second row of $J_c$ was computed by the same procedure for the $y$-direction of the

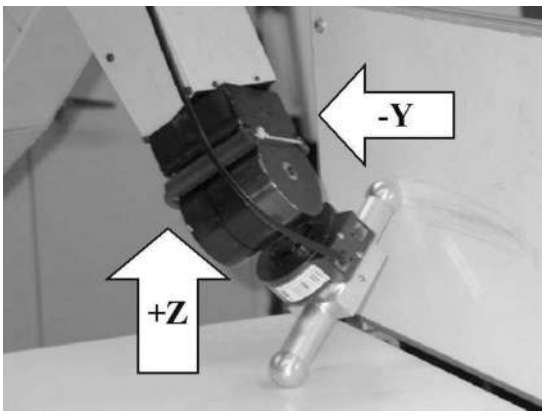


Fig. 6. System setup for multi-contact at the end-effector. Two hard contacts are made at the end-effector, one link. Experiments were conducted for multiple contact control at one link.

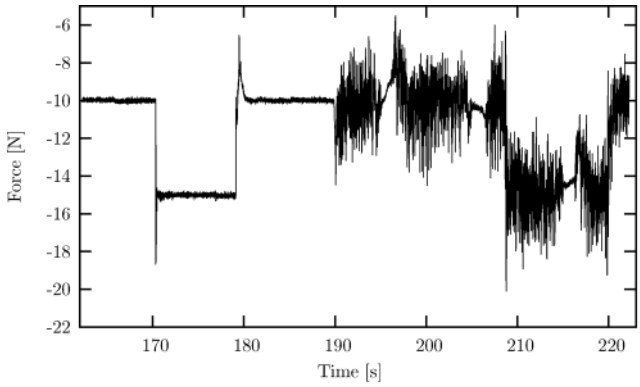


(a) Measured contact force of the first contact in $z$ direction.

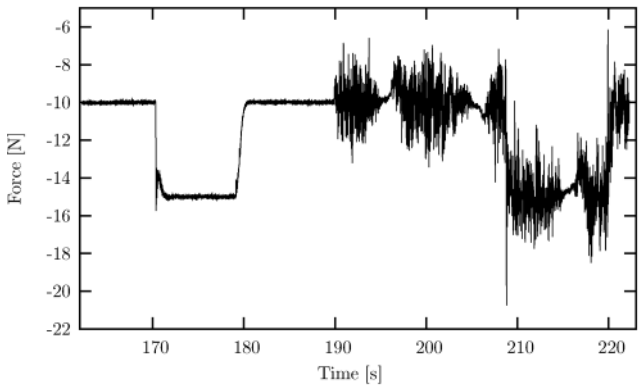


(b) Measured contact force of the second contact in $y$ direction.

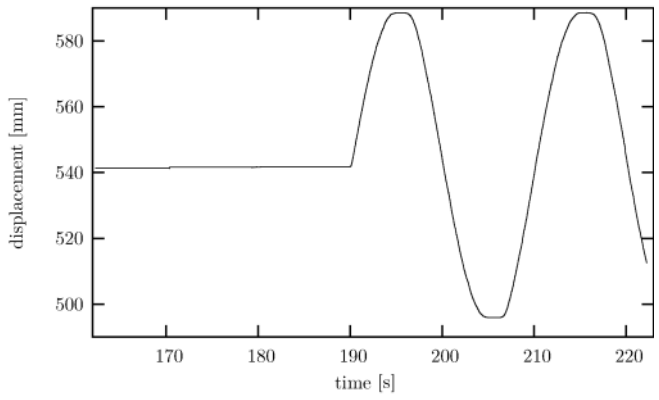


(c) Wrist translational motion in $x$ direction.

Fig. 7. Step responses of force control in case of multiple contacts at end-effector. Sinusoidal input was commanded to the wrist in the $x$ translational direction from 190 s. Refer to Fig. 6 for experimental setup. (a) Contact force with the table (first contact). (b) Contact force with the vertical board (second contact). (c) Wrist motion in null-space.

vertical board contact. The corresponding Jacobian, $J_m$, was the concatenation of the Jacobian for the orientation of the end-effector and the selected Jacobian of the wrist point along the $x$-direction in Fig. 6.

Figure 7 shows the experimental result of contact force and motion control. Square functions were commanded for the two contact forces. The $x$ direction motion of the end-effector was commanded to track a sinusoidal reference input while the orientation of the wrist was commanded to remain fixed. Since the orientation of the end-effector did not change during this motion, the contact point of the end-effector remained the same throughout the experiments.

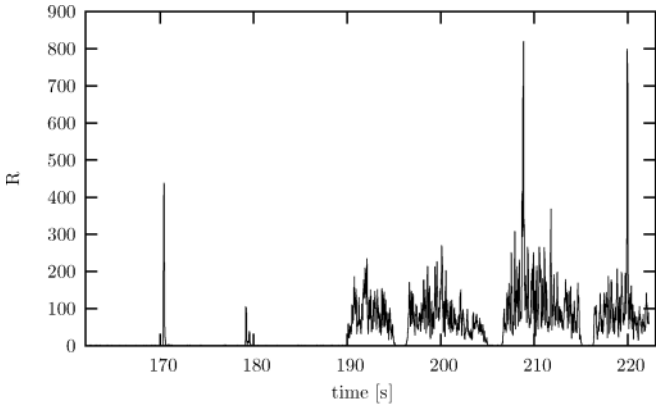


(a) Noise Covariance Estimation for the first contact force.

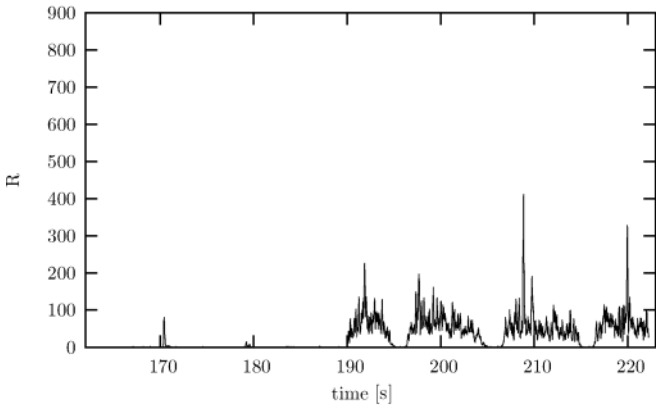


(b) Noise Covariance Estimation for the second contact force.

Fig. 8. Noise Variance Estimations of the contact forces in case of multiple contacts at end-effector. Data is from the same experiment as Fig. 7. (a) Table (first contact). (b) Vertical board (second contact).

Figures 7 (a) and (b) show the contact forces over time. The translational motion in the $x$-direction is represented in Figure 7 (c). The manipulator started with no motion (range [160–190] [s]). In this period, step commands (10 [N] and 15 [N]) had been applied simultaneously to both $z$ and $y$ directions. The operational point of the end-effector (the wrist point) started moving at 190 [s] in the $x$-direction.

The contact force reached the commanded force with the designed time constant. Figure 8 shows the force variance for each contact. The variance was about 0.6 $[N^2]$ in a static situation, increasing to about 100 $[N^2]$ when the manipulator moved. These changes in force measurement characteristics were due to the surface of the environment, along with the fact that the contact point was sliding. When the contact point moved on the surface maintaining contact, roughness in the surface created larger magnitude of noise in the measurement. Dealing with these changes in the measurement characteristic, the variance of the force measurement was computed and updated on-line using the most recent 50 samples in the experiments. Without the update, instability could easily have occurred when the contact points started to slide on the surface. When the noise characteristic varied a lot between the static and dynamic cases, the on-line noise characteristic estimation was able to properly adapt the estimation and control such that the contact forces were not too badly affected by the motion.

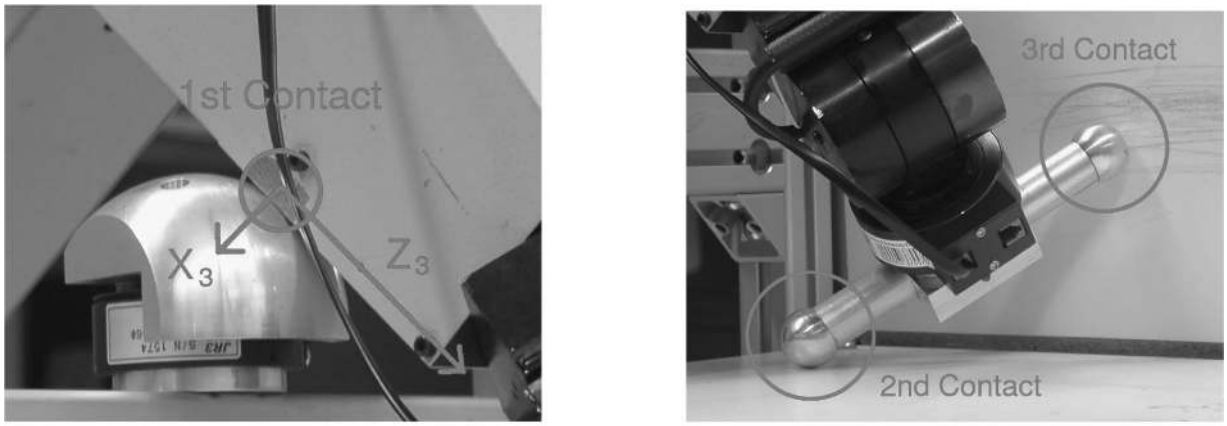


(a) (b)

Fig. 9. System setup for multi-link multi-contact. (a) Third link contact. (b) End-effector contact at two points. Motion and force control experiments were conducted for the case of multiple contacts over multiple links.

However, the starting motion of the end-effector disturbed both contact forces significantly due to static friction at about 195, 205, and 217 [s].

The value of $k_{s,i} = 6,000$ N/m was used for the stiffnesses of both the table and the vertical board. Although this value was not accurate, the robust force control with a modified Kalman estimation (AOB) compensated for modeling errors, guaranteeing the desired contact force dynamics.

*4.2. Multiple contacts over multiple links*

The experimental setup for multi-link multi-contact is shown in Fig. 9. Contact force control was for three contacts: one at the third link, and the others at the end-effector. The first contact was established at the third link, and the second and third contacts were the same as the previous experiments. For the third link contact, the contact force direction was normal to the link, i.e., $X_3$ direction in Fig. 9 (a). Therefore, the first row of the contact Jacobian, $J_c$, was the $X_3$ direction projection of the Jacobian for the contact point of the third link. The second and third rows of $J_c$ were the same as $J_c$ from the previous experiments.

Motion control was realized within the remaining three DOF of the robot through null space control. One motion task was to hold the contact position along the third link, i.e., $Z_3$ in Fig. 9 (a). Additionally, the fourth joint angle was controlled to track desired motion. The first row of $J_m$, therefore, corresponded to the motion of the third-link contact point in $Z_3$ direction and the second row was simply [0 0 0 1 0 0] for the fourth joint.

To measure the third link contact force, an additional JR3 force sensor was mounted on the contact environment since it is difficult to mount onto the link of the robot. The contact normal force can be computed by projecting the measured contact force to the normal direction of the contact surface using the kinematics and geometry of the contact link. The contact point on the link and the corresponding normal direction to the contact surface changed during the multi-contact experiments with the motion. The change of the contact location with respect to the link in the $Y_3$ direction did affect the corresponding contact Jacobian. The contact location change, therefore, needed to be accounted for in updating the contact Jacobian. The contact point with respect to the link could be estimated using the geometry of the environment and the fact that the environment was stationary.[21] The estimation of the contact point on the link and the normal direction was updated at each servo cycle.

The second and third contacts were at the end-effector; one contact with the horizontal table and the other with the vertical rigid board in Fig. 9 (b). Since the parts on the contact had a spherical shape, the contact point on the end-effector also changed when there was an orientation change at the end-effector. This exact contact location can be estimated using the kinematics of the robot and the spherical shape of the contacting part. During this experiment, the actual change of the contact location was within a couple of millimeters. Therefore, this slight change of the contact location was not accounted for but treated as a modeling error.

The contact environments were a wooden table and a wooden vertical board with aluminum frames. Consequently, they were near rigid contacts. However, the mounting between the table and the vertical board had some flexibility. The system stiffnesses of the three contacts were set to $k_{s,1} = 6,000$ N/m for the third link contact, $k_{s,2} = 6,000$ N/m for the end-effector contact with the table, and $k_{s,3} = 3,000$ N/m for the end-effector contact with the vertical board. The actual stiffnesses of all three contacts were effectively infinite at high contact forces.

Two sets of experiments were conducted with and without motion command in the null space. During the execution of motion in the null-space, the contact points were sliding on the surfaces.

(1) *Static contact experiment (Fig. 10):* While three contact forces were controlled, the motion control was commanded to maintain the starting values. Since all three contacts were very stiff, the motion of the robot was very small during the experiment. When one of the desired contact forces was commanded with square functions, the other desired contact forces were controlled to maintain their values.

Although the effect of one contact force control on the others was not perfectly eliminated, contact force control

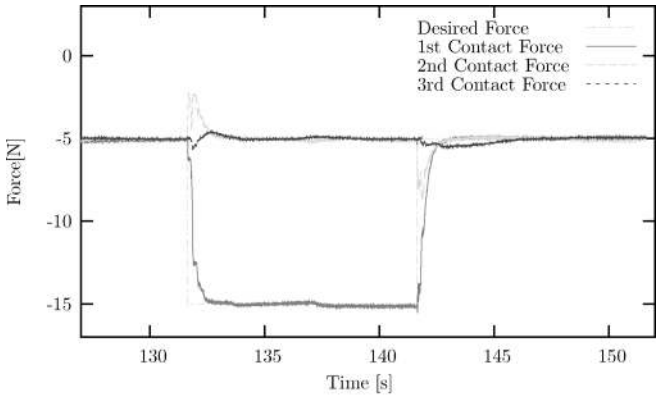


(a) Step response of contact force at third link (1st contact)

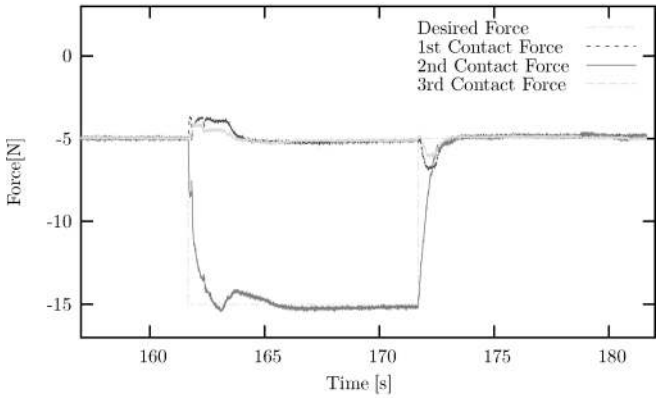


(b) Step response of contact force at end-effector with horizontal table (2nd contact)

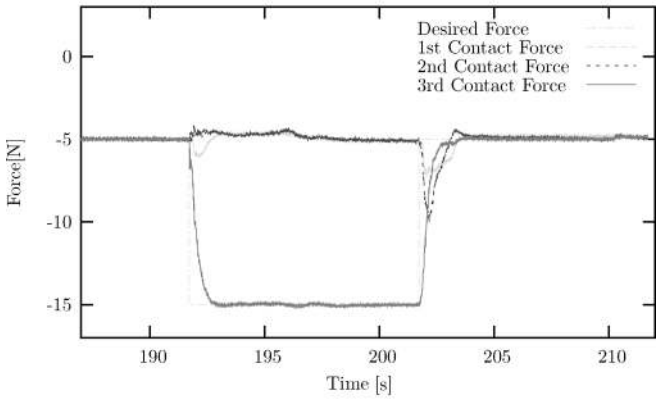


(c) Step response of contact force at end-effector with vertical board (3rd contact)

Fig. 10. Step responses of force control in case of multiple contacts at multiple links. Refer to Fig. 9 for experimental setup. Three contact forces were controlled without null-space motion. Square inputs between $-5N$ and $-15N$ were commanded to each contact and the others were commanded to maintain $-5N$. That is, a square input was commanded to the first contact in (a), to the second contact in (b), and to the third contact in (c).

was successfully accomplished. The settling time of the step response was longer than the designed value (0.23 s) mainly due to the interaction with the other contact force controls. At the time of the step command, the contact force control corresponding to the step command created disturbance to the other contact forces, whose controllers, then, compensated for the disturbance. The fact that the experimental results do not produce perfect decoupling among the contact forces are due to mainly two reasons. First, the dynamic model and the contact location of the robot are not perfect. Second, friction effects tangent to the contact surface were not accounted for. This friction is mainly nonlinear static friction or stiction in this static contact case. Even in a high stiffness environment, the robot force control generates motion and the friction can affect transient performance.

(2) *Moving contact experiment (Fig. 11):* Three contact forces were controlled to follow step commands from $-5$ to $-15$ $[N]$ and the displacement along the third link was commanded to maintain its position. Concurrently, the desired orientation of the end-effector was designed to rotate around the 4th joint of the PUMA560, i.e., the first joint of the wrist. With this null-space motion, the second and third contact points moved along the table and vertical board correspondingly. The first contact at the third link also moved in the direction that was perpendicular to the link and the contact normal direction. That is, the contact point moved in the $Y_3$ direction in Fig. 9 (a).

The coupling effect among the contact forces was aggravated by the motion of the robot in the null space. In addition to the reasons explained for the static contact experiments above (4.2.2), the motion in contact creates greater disturbances due to surface roughness and static, kinematic, and viscous friction. Static friction occurs at the beginning of motion and kinematic and viscous friction appear during motion. In fact, the direct effect of these types of friction is on the motion control. Since the design of motion control was a PD controller, those friction forces were treated as disturbance to the motion controller. However, due to the high nonlinearity of the manipulator dynamics, this disturbance on motion control affects the contact forces. A possible approach to overcome these friction effects is to estimate and compensate for the tangential friction forces. Within the accuracy of geometry information, the friction component can be extracted from the force sensor measurement. It would not only provide better decoupling in the control of contact forces and motion, but also improve performance.

## 5. Conclusion

Control for contact force and motion of a robot at multiple contacts is addressed in this paper. In the presented multicontact control framework, the operational space is composed of contact normals at each contact point. The dynamics of the robot are then used to provide a decoupled control structure for each contact force, with motion controlled in the null space of the contact force control. This new approach provides an architecture which deals with robots experiencing multiple contacts, a problem which previous approaches could not resolve. To effectively deal with modeling errors in practice, full state feedback with an active observer (AOB), is applied to each contact force control system.

This framework has been developed to deal with complex contact situations for high DOF robotic systems such as humanoid robots. These robots often encounter multiple contact situations on the hands, feet, and other links simultaneously. Experimental results from a PUMA560 manipulator demonstrate the successful implementation of this framework. The first set of experiments investigates

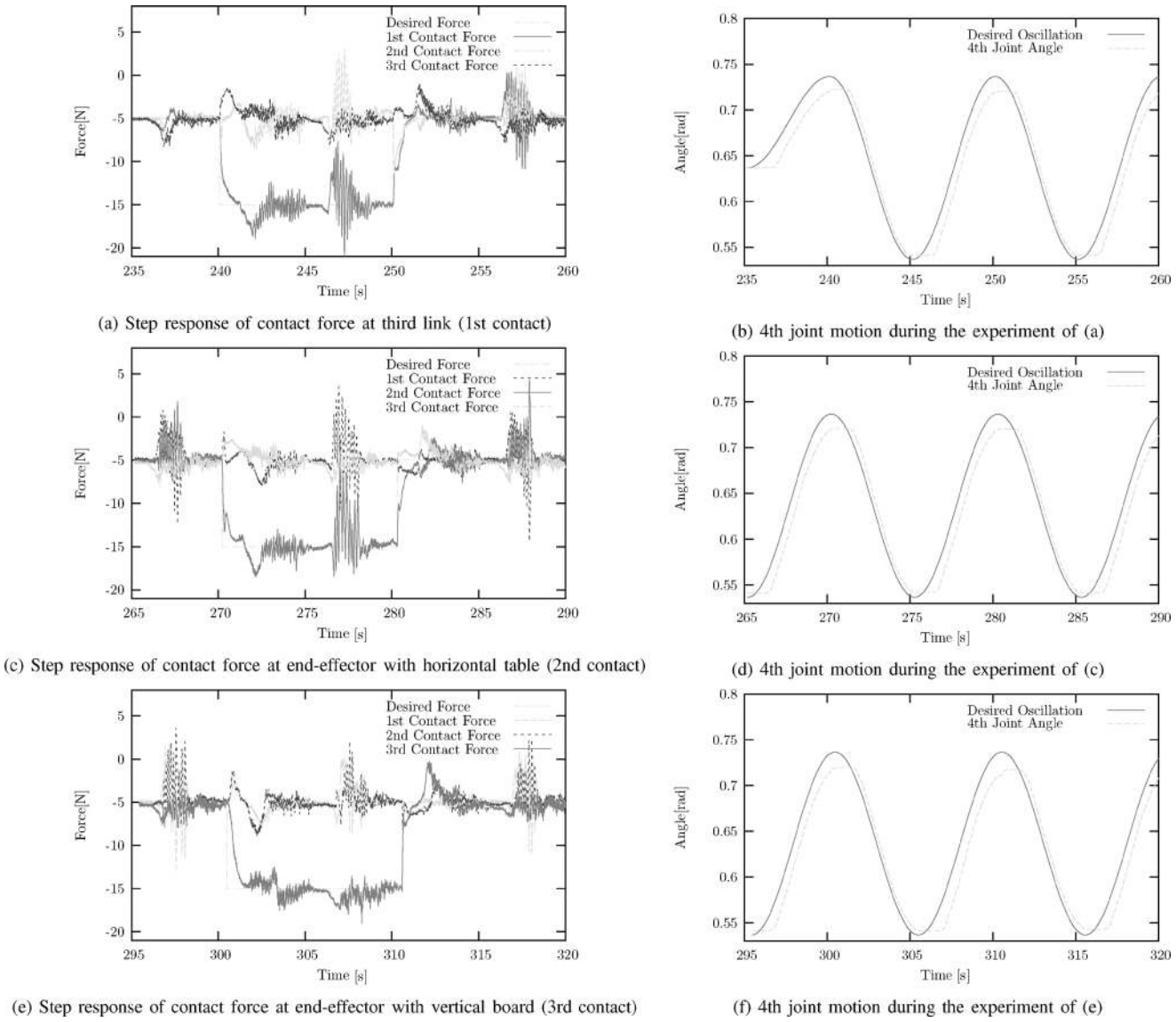


(a) Step response of contact force at third link (1st contact)

(b) 4th joint motion during the experiment of (a)

(c) Step response of contact force at end-effector with horizontal table (2nd contact)

(d) 4th joint motion during the experiment of (c)

(e) Step response of contact force at end-effector with vertical board (3rd contact)

(f) 4th joint motion during the experiment of (e)

Fig. 11. Step responses of force control in case of multiple contacts at multiple links. Refer to Fig. 9 for experimental setup. Three contact forces were controlled with null-space motion. Square inputs between $-5N$ and $-15N$ were commanded to each contact and the others were commanded to maintain $-5N$. That is, a square input was commanded to the first contact in (a) and (b), to the second contact in (c) and (d), and to the third contact in (e) and (f). The 4th joint was simultaneously controlled in the null-space, following a sinusoidal trajectory.

contact with the environment at two points on the end-effector, and the second set of experiments addresses three point contact: one at the third link and two at the end-effector. Static and moving contact experiments show the high performance of the multi-link multi-contact force control framework even in the presence of varying contact characteristics and disturbance from the motion of the manipulator. Currently, the framework is being implemented and validated on a humanoid system, HONDA ASIMO, in the Stanford AI laboratory.

## References

1. H. Ambrose and Z. Qu, "Model Reference Robust Control for Mimo Systems," *Proceedings of the American Control Conference*, Albuquerque, New Mexico (1997) pp. 345–349.
2. A. Bicchi and V. Kumar, "Robotic Grasping and Contact: A Review," *Proceedings of the International Conference on Robotics and Automation*, San Francisco, U.S.A. (2000) pp. 348–353.
3. H. Bruyninckx, S. Demey, S. Dutré and J. De Schutter, "Kinematic models for model-based compliant motion in the presence of uncertainty," *Int. J. Robot. Res.* **14**(5), 465–482 (Oct. 1995).
4. K. Chang and O. Khatib, "Manipulator Control at Kinematic Singularities: A Dynamically Consistent Strategy," *Proceedings of the International Conference on Intelligent Robots and Systems*, Pittsburgh, U.S.A. (1995) pp. 84–88.
5. S. Chiaverini, B. Siciliano and L. Villani, "A Survey of Robot Interaction Control Schemes with Experimental Comparison," *ASME Trans. Mechatronics* **4**(3), 273–285 (Sep. 1999).
6. R. Cortesão, Kalman Techniques for Intelligent Control Systems: Theory and Robotic Experiments. *Ph.D. thesis* (University of Coimbra, 2002).
7. R. Cortesão, J. Park and O. Khatib, "Real-Time adaptive control for haptic telemanipulation with kalman active observers," *IEEE Trans. Robot.* **22**(5), 987–999, 2006.
8. R. Featherstone, S. S. Thiebaut and O. Khatib, "A General Contact Model for Dynamically-Decoupled Force/Motion

Control," *Proceedings of the International Conference on Robots and Automation*, Detroit, U.S.A. (1999) pp. 3281–3286.
9. E. Freund, "The structure of decoupled nonlinear systems," *Int. J. Control*, **21**(3), 443–450 (1975).
10. C. D. Johnson, "Discrete-time disturbance-accommodating control theroy with applications to missile digital control," *J. Guid. Control* **4**(2), 116–125 (1980).
11. O. Khatib, "A unified approach for motion and force control of robot manipulators: The operational space formulation," *Int. J. Robot. Autom.* **3**(1), 43–53 (Feb. 1987).
12. O. Khatib and J. Burdick, "Motion and Force Control of Robot Manipulators," In: *Proceedings of the International Conference on Robotics and Automation*, San Francisco, U.S.A. (1986) pp. 1381–1386.
13. O. Khatib, L. Sentis, J. Park and J. Warren, "Whole-body dynamic behavior and control of human-like robots," *Int. J. Humanoid Robot.* **1**(1), 29–43 (2004).
14. H. Lipkin and J. Duffy, "Hybrid twist and wrench control for a robotic manipulator," *ASME J. Mech. Trans. Autom. Des.* **110**(2), 138–144 (Jun. 1988).
15. Y. Liu, K. Kitagaki, T. Ogasawara and S. Arimoto, "Model-based adaptive hybrid control for manipulators under multiple geometric constraints," *IEEE Trans. Control Sys. Technol.* **7**(1), 97–109 (Jan. 1999).
16. K. Mirza and D. E. Orin, "Control of Force Distribution for Power Grasp in the Digits System," *Proceedings of the Conference on Decision and Control*, Honolulu, Hawaii, U.S.A. (1990) pp. 1960–1965.
17. Y. Nakamura and H. Hanafusa, "Inverse Kinematic Solutions with Singularity Robustness for Robot Manipulator Control," *ASME J. Dyn. Syst. Meas. Control*, **108**(3), 163–171 (1986).
18. J. Park, R. Cortesão and O. Khatib, "Multi-Contact Compliant Motion Control for Robotic Manipulators," *Proceedings of the International Conference on Robotics and Automation*, New Orleans, U.S.A. (2004) pp. 4789–4794.
19. J. Park and O. Khatib, Mult-link Multi-contact Force Control for Manipulators. In *Proceedings of the International Conference on Robotics and Automation*, Barcelona, Spain (2005) pp. 3613–3618.
20. Jaeheung Park and Oussama Khatib, "A haptic teleoperation approach based on contact force control," *Int. J. Robot. Res.* **25**(5–6), 575–591 (2006).
21. A. Petrovskaya, J. Park and O. Khatib, "Probabilistic Estimation of Whole Manipulator Contacts for Multi-contact Control," *Proceedings of the International Conference on Robotics and Automation*, Rome, Italy (2007).
22. M. H. Raibert and J. J. Craig, "Hybrid position/force control of manipulators," *ASME J. Dyn. Sys. Meas. Control* **103**(2), 126–133 (June 1981).
23. J. Russakow, O. Khatib and S. M. Rock, "Extended Operational Space Formulation for Serial-to-parallel Chain(branching) Manipulators," *Proceedings of the International Conference on Robotics and Automation*, Nagoya, Japan (1995) pp. 1056–1061.
24. K. Salisbury, W. Townsend, B. Eberman and D. DiPietro, "Preliminary Design of a Whole-arm Manipulation System (wams)," In: *Proceedings of the International Conference on Robotics and Automation*, Philadelphia, PA, U.S.A. (1988) pp. 254–260.
25. J. De Schutter, J. Rutgeerts, E. Aertbeliën, F. De Groote, T. De Laet, T. Lefebvre, W. Verdonck and H. Bruyninckx, "Unified Constraint-Based Task Specification for Complex Sensor-Based Robot Systems," In: *Proceedings of the International Conference on Robotics and Automation* Barcelona, Spain (2005) pp. 3607–3612.
26. B. Siciliano and L. Villani, Robot Force Control, "The Kluwer International Series In Engineering and Computer Science." (Kluwer Academic Publishers, 1999).
27. C. W. Wampler, "Manipulator inverse kinematic solutions based on vector formulations and damped least-squares methods," *IEEE Trans. Sys. Man Cybern.* **16**(1), 93–101 (1986).
28. H. West and H. Asada, A Method for the Design of Hybrid Position/Force Controllers for Manipulators Contrained by Contact with the Environment," *Proceedings of the International Conference on Robotics and Automation* (1985) pp. 251–259.
29. T. Yoshikawa, "Force Control of Robot Manipulators," *Proceedings of the International Conference on Robotics and Automation* San Francisco, USA (2000) pp. 220–226.
30. Y. Zhang and W. A. Gruver, "Definition and Force Distribution of Power Grasps," In: *Proceedings of the International Conference on Robotics and Automation* Nagoya, Japan (1995) pp. 1373–1378.